Structural and electronic properties of Li- and Cu-doped β-rhombohedral boron constructed from icosahedral and truncated icosahedral clusters

H. Matsuda, T. Nakayama, and K. Kimura

Department of Materials Science, University of Tokyo, Tokyo 113, Japan

Y. Murakami* and H. Suematsu

Department of Physics, University of Tokyo, Tokyo 113, Japan

M. Kobayashi and I. Higashi

Institute of Physical and Chemical Research (RIKEN), Saitama 351-01, Japan

This study performs dc conductivity and static magnetic-susceptibility measurements on Li- and Cu-doped β-rhombohedral boron (β-rhombohedral B), which is a unique polymorphic semiconducting (group III) material composed of B_{12} icosahedral clusters. dc conductivity results show a variable-range-hopping (VRH)-type temperature dependence with a typical localization length of about ~ 1 Å. In addition, the density of states (DOS) at the Fermi energy, which is calculated from fitted parameters of VRH conduction, was found to have a peak with respect to metal concentration, such that at the highest concentration ($Li_{7.9}B_{105}$ and $Cu_{4.2}B_{105}$), metal-doped β-rhombohedral B appears to revert back to an insulator, instead of showing insulator-to-metal transition. Corresponding static magnetic-susceptibility results, however, show a contribution from Pauli paramagnetism in the temperature-independent component χ_0, where a similar concentration dependence is shown to that in the DOS of VRH conduction. Based on these properties, we discuss the possibility of filling the intrinsic acceptor band, which originates from the uppermost molecular bonding orbital of the B_{12} icosahedral cluster that is split by the Jahn-Teller effect. β-rhombohedral B's crystalline structure can also be viewed as a slightly distorted face-centered cubic (fcc) packing of B_{84} soccer-ball-shaped clusters covalently bound to each other and containing a relatively large number of large-size interstitial doping sites. This structure is considered to be topologically similar to that of fcc C_{60}, although the bonding mechanisms of their clusters are different, and therefore we also describe the similarities and differences between them.

I. INTRODUCTION

Crystalline boron-rich solids are unique elemental (group III) semiconductors possessing several complex structures reflecting their unique bonding nature, i.e., a three-center covalent bond between three mutually-adjacent B_{12} icosahedral clusters [Fig. 1(a)] and a packing comprised of these clusters. Such crystalline structures produce the outstanding electronic properties of boron-rich solids.[1] Each B_{12} cluster has 12 intericosahedral bonding orbitals along its fivefold axes, accommodating 12 electrons when it forms conventional pair bonds with 12 neighboring B_{12} clusters. They also contain 13 intraicosahedral bonding orbitals that accommodate 26 electrons. Thus, 38 electrons are necessary to fill all these bonding orbitals, though only 36 ($= 3 \times 12$) valence electrons are available. Consequently, due to the deficiency of valence electrons and the Jahn-Teller effect, a B_{12} cluster may be distorted such that the uppermost, normally fourfold degenerated intraicosahedral bonding orbitals of an ideal icosahedron may have its unoccupied states separated from the occupied ones.[2] It is thought that this unoccupied orbital leads to an intrinsic acceptor band above the valence-band edge in β-

rhombohedral boron solids (β-rhombohedral B or B_{105}, the most popular structure among the four known polymorphic icosahedral pure-boron semiconductors). This acceptor band is partially occupied by the electrons from other forms of boron clusters, and has been detected by optical absorption measurements.[3] The crystalline structure of β-rhombohedral B is a distorted face-centered cubic (fcc) lattice of B_{84} soccer-ball-shaped clusters constructed with B_{12} icosahedral clusters [Fig. 1(b)], being topologically similar to that of another elemental semiconductor, fcc C_{60}, which is a recently discovered, superconducting host material that has attracted much research attention.[4-6] fcc C_{60} has a crystalline framework comprised of an fcc lattice of C_{60} truncated icosahedral molecules (soccer-ball-shaped clusters), and it shows a transition to the superconducting state up to 33 K. fcc C_{60} has also shown metallic properties of conduction electrons at the normal state upon charge transfer from alkaline and alkaline-earth metals to C_{60} molecules. In related work, Kawaji *et al.*[7] recently reported on the superconductivity of Ba- and Na-doped $Na_2Ba_6Si_{46}$, while Saito and Oshiyama[8] calculated electronic structures of pristine solid Si_{46} and $Na_2Ba_6Si_{46}$, both of which have a crystalline structure that is essentially a body-centered cubic lattice (bcc) of Si_{20} or Na@Si_{20} (Na@Si_{20} denotes

an endohedral cluster) dodecahedra connected to each other by covalent bonds. According to their calculation, pristine solid Si_{46} is also an elemental semiconductor having a wider energy gap than that of diamond-structured solid Si, though in both solids, the Si atoms are tetrahedrally coordinated. In the calculation for $Na_2Ba_6Si_{46}$, charge transfer occurs from the Na atoms to Si_{20} cages, as does hybridization between Ba states and Si_{46} conduction states, which lead to forming a metallic electronic structure similar to that in metal-doped C_{60} solids. Thus, we postulate that these solids are similar because (i) they are all packed with clusters possessing icosahedral symmetry (nearly spherical clusters), and (ii) they contain a relatively large number of large-size interstitial doping sites. After considering the similarities and relationships among these semiconductors, we decided it

would be of value to investigate the physical properties of electron- and hole-doped β-rhombohedral B and compare them with those of fcc C_{60} and solid Si_{46}. It is realized, of course, that their electronic structures and physical properties may be quite different, since the clusters share covalent bonds in β-rhombohedral B and Si_{46}, whereas in fcc C_{60} they share van der Waals bonds, and also since the characteristic clusters among these solids are different.

We selected Li metal as a donor, because in most conventional group IV and III-V semiconductors, the interstitial Li atoms form shallow donor levels on the same order as substitutional impurities. In addition, after Li doping, it is possible to theoretically predict the metallic properties and superconducting transition of the other form of crystalline pure boron (α-rhombohedral
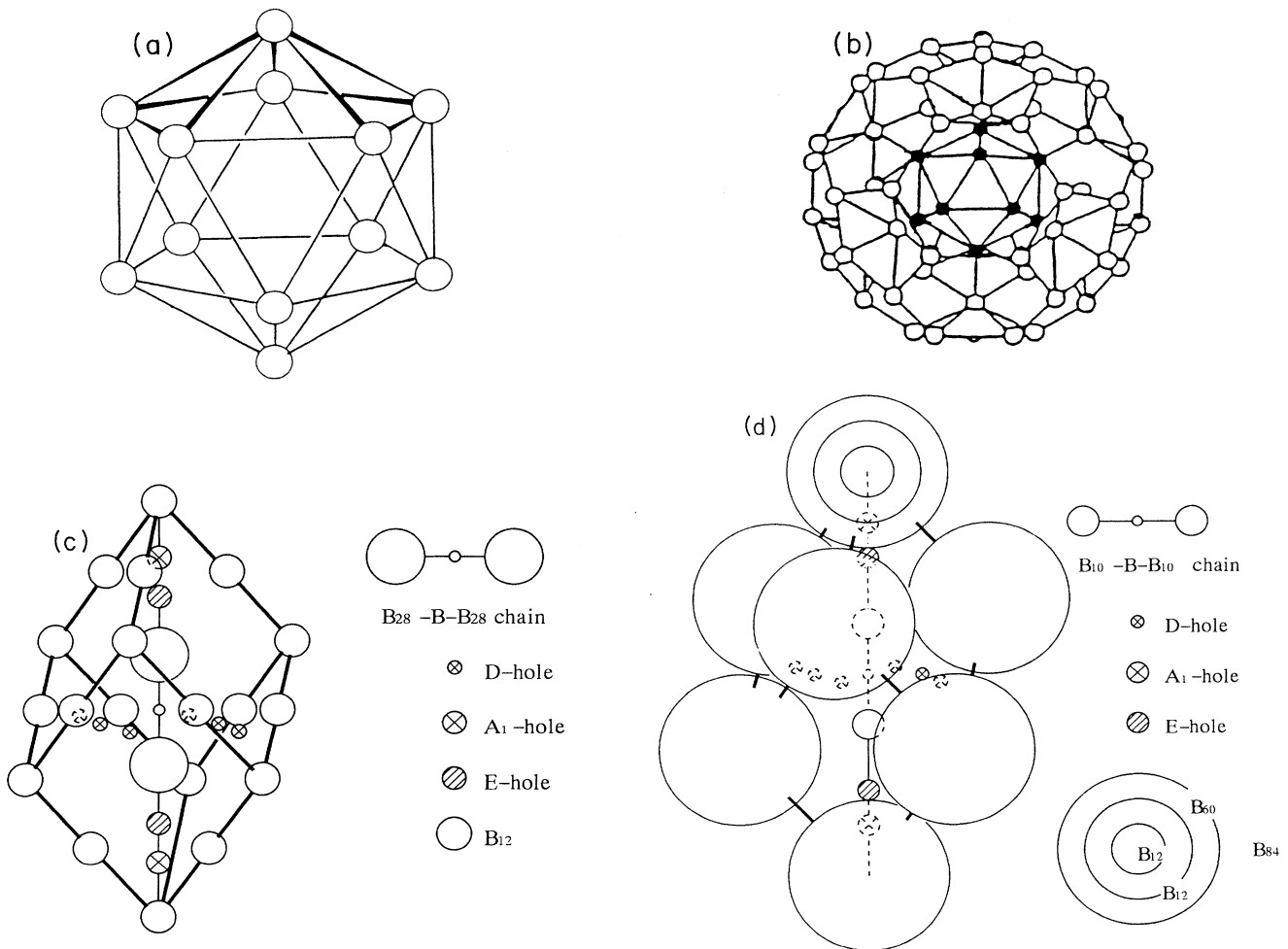
FIG. 1. (a) B_{12} icosahedral cluster. (b) B_{84} soccer-ball-shaped cluster in β-rhombohedral B, where two B_{12} icosahedra are concentrically inserted into a B_{60} soccer-ball-shaped cage. (c) Crystalline structure of β-rhombohedral B, where B_{12} icosahedra occupy the vertices and edge centers of a rhombohedral unit cell, and a B_{28} cluster, which is a modified trio comprised of B_{12} icosahedra, a single boron atom B, and another B_{28} cluster are situated in series (B_{28}-B-B_{28} chain) along the main body diagonal. Distributions of the major doping sites are also shown (Ref. 13). (d) Another view of β-rhombohedral B, where a B_{84} soccer-ball-shaped cluster occupies each vertex of the rhombohedral unit cell and a B_{10}-B-B_{10} chain occupies the main body diagonal.

B),[9] which in comparison, possesses a slightly distorted fcc packing of B_{12} icosahedra. Regarding hole doping with Cu, we did so because calculations to determine the impurity level positions of interstitial $3d$ transition metals in Si suggest that these level positions approach closer to the valence band of Si with increasing atomic number,[10] and therefore, Cu atoms may form their acceptor level,[11] and in fact, the sign of the Seebeck coefficient for Cu-doped β-rhombohedral B is positive for any Cu concentration.[12] The present study reports on the structural and electronic properties of this Li electron- and Cu-hole-doped β-rhombohedral B material.

II. EXPERIMENT

To interstitially dope Li atoms into β-rhombohedral B, polycrystalline β-rhombohedral B (99% pure powder, though some bits were at 99.9%) and Li metal (99.9% pure) were placed at both ends of a tantalum cell that was then sealed. This was done to prevent Li from reacting with the glass reaction tube. After evacuating and sealing the cell in the tube, it was heated at 900-1000 °C for 24 to 140 h until the vapor reaction occurred. To obtain Cu-doped β-rhombohedral B, Cu powder (99.9% pure) and B powder (99.9% pure) were mixed together and melted in an arc discharge furnace under an Ar atmosphere. To homogenize the resultant alloy, it was annealed at 900 °C for 48 h under an Ar atmosphere. Since Al metal was added to vary the Cu concentration of single-crystalline specimens, we also investigated the properties of Cu- and Al-doped single crystals precipitated from B, Cu, and Al melts. As previously described, structural refinements were performed on single-crystalline Cu-doped β-rhombohedral B[13] and polycrystalline Li-doped β-rhombohedral B.[14]

To determine the final concentrations of Li (x; Li_xB_{105}) and Cu (y; Cu_yB_{105}) using changes in the unit-cell volume, we employed x-ray powder diffraction (XRD) analysis. Composition and lattice parameter measurements taken during the structural refinements were used as the standard values. Inductively coupled plasma (ICP) analyses were also performed to obtain metal concentrations. dc conductivity was measured from 30 to 300 K per the van der Pauw method, while the magnetic susceptibility was measured from 2 to 300 K under a magnetic field of 1 T using a superconducting quantum interference device magnetometer (Quantum Design). The magnetization process was also measured at 5 and 300 K under various magnetic fields (maximum of 5 T).

III. RESULTS AND DISCUSSION

A. Structure and doping sites

The rhombohedral unit cell of β-rhombohedral B [Fig. 1(c)] contains 105 boron atoms[15] dispersed among the following structural components: (i) two kinds of B_{12} icosahedra respectively situated at the vertices and edge centers, being covalently connected to each other along one of their fivefold axes, and (ii) a B_{28} cluster, which is a modified trio comprised of B_{12} icosahedra, a single boron atom B, and another B_{28} cluster situated in series (B_{28}-B-B_{28} chain) along the main body diagonal of the rhombohedron. The structure of the unit cell can also be viewed as follows: (i) a B_{84} soccer-ball-shaped cluster [Fig. 1(b)] occupies each vertex of the rhombohedron such that it is covalently connected to 12 B_{84} clusters [Fig. 1(d)], and (ii) a B_{10}-B-B_{10} chain occupies the main body diagonal, which is formed if three half fragments of B_{12} are clipped off each end of a B_{28}-B-B_{28} chain. The B_{84} soccer-ball-shaped structure is formed by a B_{12} situated at a vertex of the rhombohedron and 12 neighboring half fragments of B_{12} situated at the edge centers, i.e., two boron icosahedra are concentrically inserted into a B_{60} soccer-ball-shaped cage. Note that the main framework of this crystalline structure is a distorted fcc lattice comprised of a B_{84} soccer-ball-shaped cluster, and therefore, the structure is topologically similar to that of fcc C_{60}.

Table I summarizes the structural parameters of the rhombohedral unit cell for β-rhombohedral B and fcc C_{60}, where the distance between the centers of the B_{84} soccer-ball-shaped clusters in β-rhombohedral B is almost the same as the corresponding distance in fcc C_{60} ($\sim$ 10 Å), though the radius of the former cluster is comparatively larger due to the two inner icosahedra ($B_{60}+2\times B_{12}$). This structural difference results in the surfaces of the β-rhombohedral B clusters being closer together, which may be the reason that β-rhombohedral B clusters share covalent bonds, whereas those in fcc C_{60} share weaker van der Waals bonds.

The distribution and dimensions of the doping sites in the rhombohedral unit cell of β-rhombohedral B are shown in Figs. 1 and 2, respectively. For comparison, Fig. 2 also shows the site diameters in fcc C_{60}, which has one octahedral and two tetrahedral doping sites in its rhombohedral primitive cell. Note that the E hole of β-rhombohedral B [Figs. 1(c) and 1(d)), which is related to the tetrahedral site in an fcc lattice, has a similar size as fcc C_{60}'s. Although β-rhombohedral B's octahedral site is occupied by the B_{10}-B-B_{10} chain, the D holes nevertheless encircle the center B atom as shown in Figs. 1(c) and 1(d). Furthermore, two additional sites of β-rhombohedral B, being A_1 holes, are on the main body diagonal of the rhombohedron such that each of them can be considered to be situated either at the center of a tetrahedron of B_{12} icosahedra or inside the B_{84} soccer-ball-shaped cluster.

After making the structure refinements to single-crystalline Cu- and Al-doped β-rhombohedral B,[13] A_1

TABLE I. Structural parameters of the rhombohedral unit cell in β-rhombohedral B and fcc C_{60}.

	β-rhombohedral B	fcc C_{60}
Lattice angle α (deg)	65.18	60.00
Lattice constant a (Å)	10.14	9.93
Soccer-ball-shaped cluster radius R (Å)	4.64	3.55
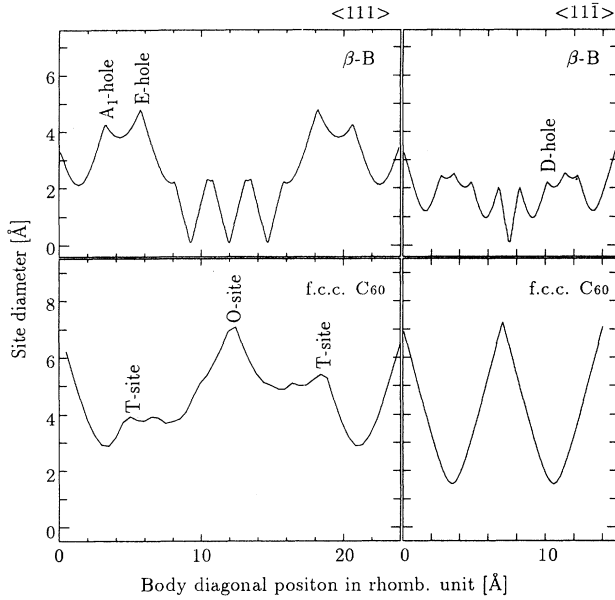
FIG. 2. The diameters of doping sites along the body diagonal of the β-rhombohedral B or fcc C_{60} rhombohedral unit cell. These correspond to twice the smallest distance between the lattice points and body diagonals of the rhombohedra after subtracting the diameters of atoms as determined using the covalent bond lengths (indexed with respect to the rhombohedral basis).

and E holes are not simultaneously occupied. In addition, when Al atoms are introduced, the occupancy of E holes drops to zero, whereas when Al atoms are absent, Cu atoms occupy E holes even though the A_1 hole is smaller than the E hole. In other words, A_1 holes are preferentially occupied with Al atoms. D holes, on the other hand, are occupied with both Cu and Al atoms. At the maximum Cu solubility that occurs in $Cu_{4.2}B_{105}$; E, D , and A_1 holes are, respectively, occupied with 1.2, 2.8, and 0.2 Cu atoms. Following structural refinement to $Li_{8.0}B_{105}$, Li atoms occupy every E (2) and D hole (6), but leave the A_1 holes vacant.[14] We postulate that the Li concentration in β-rhombohedral B may be saturated at

this composition. In contrast to most other metal impurities in β-rhombohedral B, which retain partial occupation of the doping sites at their maximum solubilities,[16] alkaline-metal Li atoms completely occupy all the doping sites: a fact that indicates the stoichiometric compound Li_8B_{105} exists as in K_3C_{60}, Li_2CsC_{60}, and $Na_2Ba_6Si_{46}$.

Table II shows resultant XRD-determined lattice dimensions of the β-rhombohedral B rhombohedral unit cell as the metal concentrations are varied. The observed XRD patterns for Li- and Cu-doped samples indicate the β-rhombohedral B structure is slightly shifted due to lattice expansions caused by interstitially introducing the metal atoms. Consequently, the final concentrations of doped Li (x) and Cu (y) were determined by interpolating between the unit-cell volume for polycrystalline $Li_{8.0}B_{105}$ and single-crystalline $Cu_{4.2}B_{105}$, respectively, as well as for polycrystalline β-rhombohedral B of $3N$ purity. Note that the indicated ICP results are quite similar to those obtained by XRD, though slightly higher. This may occur because the Li metal, which was not interstitially doped into β-rhombohedral B, was detected by ICP analysis.

B. Electrical conductivity

Figure 3 shows the temperature dependence of dc conductivity $[\sigma(T)]$ for (a) polycrystalline Li-doped β-rhombohedral B and (b) Cu-doped β-rhombohedral B, where, after Li or Cu doping of several at.%, $\sigma(T)$ increases by several orders of magnitude, though still being similar to that of a semiconductor. In contrast, after metal doping with several at.%, the conductivity of alkali-metal–doped fcc C_{60} loses the semiconducting behavior of pristine fcc C_{60}, and subsequently shows metallic behavior.[4,17–21] Note that fcc C_{60}'s orientational disorder in molecular alignments has been suggested to be responsible for the fact that correction of localization reduces the density of states (DOS) of the conduction band.[22] Also, as shown in Fig. 3, $\sigma(T)$ for pristine and metal-doped β-rhombohedral B reveals three-dimensional variable-range-hopping (VRH)-type behavior (Mott's law) at somewhat high temperatures (30–

TABLE II. Lattice dimensions and metal concentrations of Li- and Cu-doped β-rhombohedral B. Concentrations were determined by ICP analyses and XRD.

a (Å)	α (deg)	V_R (Å^3)	x, y (ICP)	x, y (V_R)
10.128	65.695	825.4		$Li_{1.6}B_{105}$
10.153	65.336	826.1		$Li_{2.0}B_{105}$
10.183	65.297	832.7		$Li_{5.7}B_{105}$
10.207	65.011	834.2		$Li_{6.3}B_{105}$
10.166	65.806	836.5	$Li_{9.3}B_{105}$	$Li_{8.0}B_{105}$ (standard) (Ref. 14)
10.131	65.231	819.1		$Cu_{0.1}B_{105}$
10.138	65.225	820.7		$Cu_{0.2}B_{105}$
10.139	65.199	823.2		$Cu_{0.3}B_{105}$
10.151	65.107	825.0		$Cu_{1.0}B_{105}$
10.158	65.251	827.3		$Cu_{1.9}B_{105}$
10.164	65.309	834.3		$Cu_{4.7}B_{105}$
10.189	65.226	833.1	$Cu_{4.8}B_{105}$	$Cu_{4.2}B_{105}$ (standard) (Ref. 13)
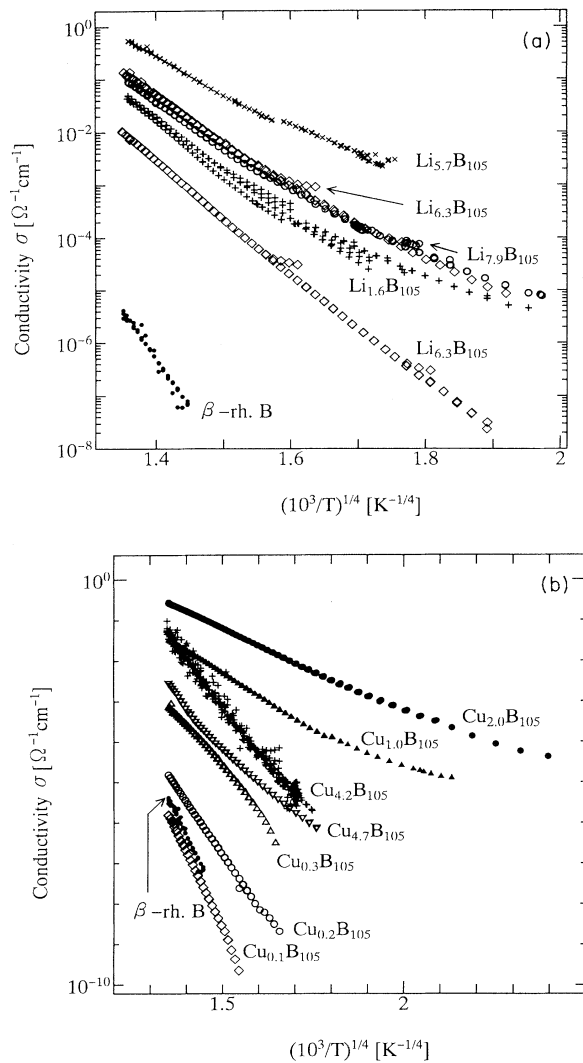
FIG. 3. Temperature dependence of dc conductivity for (a) Li-doped β-rhombohedral B polycrystals and (b) arc-melted Cu-doped β-rhombohedral B polycrystals (except for single-crystalline $Cu_{4.2}B_{105}$).

300 K). In fact, Cu- and Al-doped β-rhombohedral B single crystals still show similar temperature-dependent VRH conduction to that shown in arc-melted Cu-doped β-rhombohedral B polycrystals.[23] Therefore, such temperature dependence may not arise due to some kind of granularity effect, but instead reflect the electronic structure of β-rhombohedral B. Since $\sigma(T)$ is only slightly dependent on the Al concentration, while being more so on the Cu concentration, this may indicate that the Al atoms form other covalent bonds such that they barely contribute to affecting electronic conduction. It should be noted that this type of VRH conduction has been commonly observed in boron-rich solids: metal-doped β-rhombohedral B,[24] boron carbide,[25] and YB_{66}.[26] Another interesting fact is that Na-doped solid Si_{136} (isomorphic to solid Si_{46}) shows VRH conduction in a similar temperature range (80–400 K),[27] though an insulator-to-

metal transition occurs after further Na doping.

Since interstitially doped Li atoms form shallow donor levels in crystalline Si, we assumed that Li atoms in β-rhombohedral B are donors of monovalence. On the other hand, since the Seebeck coefficient for Cu-doped β-rhombohedral B retains a positive value,[12] it seems reasonable to hypothesize that doped Cu atoms may be acceptors of monovalence. If the intrinsic acceptor band is already almost fully occupied for pristine β-rhombohedral B, as observed in conventional semiconductors, VRH conduction may occur due to the electrons occupying Li's donor band or by the holes occupying Cu's acceptor band. Alternatively, the nearly empty intrinsic acceptor band in pristine β-rhombohedral B may create a special situation, i.e., (i) doped electrons from Li atoms may occupy the intrinsic acceptor band and show VRH conduction between localized states of the band, or (ii)
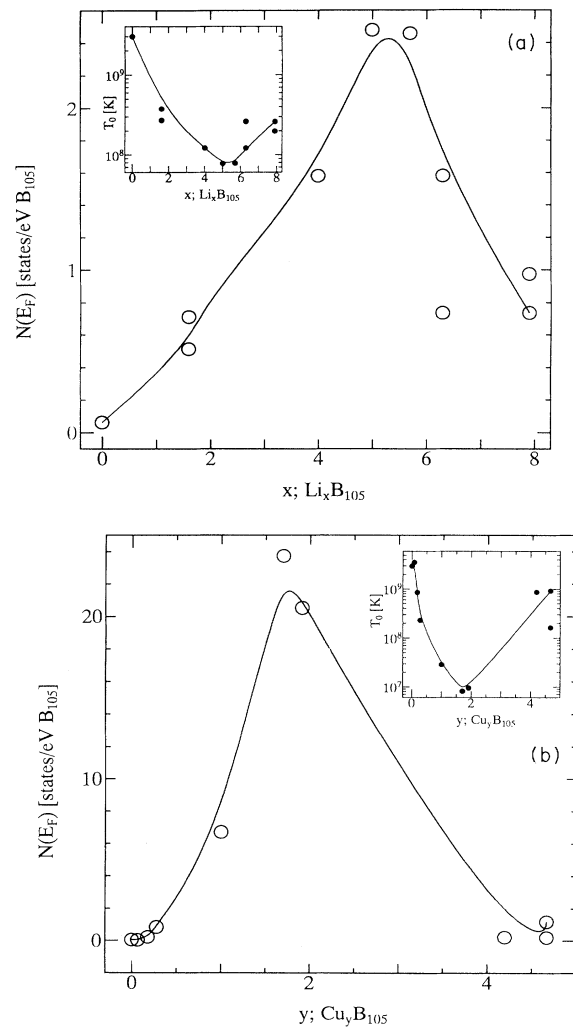
FIG. 4. Calculated DOS at the Fermi energy $N(E_F)$ derived from VRH-type dc conductivity for (a) Li-doped β-rhombohedral B polycrystals and (b) arc-melted Cu-doped β-rhombohedral B polycrystals. Inset shows the dependence of the exponential factor T_0 on the indicated concentration. The solid lines assist viewing.

Cu's acceptor band may be located between the valence band edge and intrinsic acceptor band, and therefore, VRH conduction of holes may subsequently occur in Cu's acceptor band.

According to Mott's law[28] of VRH conduction, σ is expressed as

$$\sigma = \sigma_0 \exp\left[-(T_0/T)^{1/4}\right],$$

$$T_0 = \frac{60\alpha^3}{\pi N(E_F)k_B},$$

where α^{-1} is the localization length of the wave function of the carrier and $N(E_F)$ is the density of states at the Fermi energy. Figure 4 shows the dependence of $N(E_F)$ on the Li (x) or Cu (y) concentration, while the indicated insets show the corresponding dependence of T_0. Note that T_0 for pristine β-rhombohedral B is 4×10^9 K, though its minimum value at $y = 2$ is still high at $\sim 10^7$ K. This anomalously high T_0 may indicate that Li- and Cu-doped β-rhombohedral B has a low probability of reaching insulator-to-metal transition. If we assume that several at.% of metal doping results in accommodating carriers at a density much greater than 10^{21} cm^{-3}, then the critical density for an insulator-to-metal transition n_c could surpass 10^{22} cm^{-3}. The relationship between α^{-1} and n_c can be expressed by the Mott criterion,[29] i.e.,

$$n_c^{1/3}\alpha^{-1} \simeq 0.25,$$

which yields $\alpha^{-1} \sim 1$ Å. However, as such it is much less than that possible for metal-doped crystalline semiconductors. Therefore, this may indicate that conduction does not occur in the shallow impurity levels as in conventional crystalline semiconductors, instead occurring in the deep impurity levels as in metal-doped amorphous semiconductors. If $\alpha^{-1} = 1$ Å is assumed to apply to all samples, then the dependence of $N(E_F)$ on x and y can be estimated as shown in Figs. 4(a) and 4(b), where up to $x \simeq 5$ and $y \simeq 2$, $N(E_F)$ increases. At these concentrations, doped metal atoms may donate charge carriers; i.e., Li donates electrons and Cu donates holes. Then, with an increase in either concentration, $\sigma(T)$ and thus $N(E_F)$ decrease, which is also in contrast to the behavior of conventional crystalline semiconductors, namely, with increasing impurity concentration, σ keeps increasing, and at n_c, these originally semiconducting materials are transformed to metals having a value of $T_0 = 0$ K. If the band width where hopping conduction occurs is assumed to be ~ 0.2 eV, and at $y = 2$ there exist two extra carriers in β-rhombohedral B, then $N(E_F) = 2/0.2 = 10$ [states/eV B$_{105}$], which is in good agreement with the $N(E_F)$ value obtained from T_0 after Cu doping. On the other hand, the corresponding estimated $N(E_F)$ value for Li doping is $1/10$ less than $N(E_F) = 10$. Since Li$_8$B$_{105}$ may have a stoichiometric phase (Sec. III A), and at $x > 5$ the measured conductivity (Fig. 3) starts to decrease, then the Li$_8$B$_{105}$ phase can possibly be an insulator. In other words, each B$_{105}$ unit cell may have eight electronic states in its intrinsic acceptor band, since each B$_{12}$ cluster may have one uppermost unoccupied

level that has split off and four clusters comprise a unit cell. If this band is in pristine β-rhombohedral B and it is initially empty, then at $x = 8$ the band is completely occupied with valence electrons from the Li atoms such that this phase is an insulator. Accordingly, at $x = 4$ (intermediate doping), the material may decompose into the insulator phase (Li$_8$B$_{105}$) and Li-doped β-rhombohedral B, which would then make the observed decrease in conductivity possible. Thus, $N(E_F)$ would be less than that estimated using the Li concentration. After Cu doping of β-rhombohedral B, since the observed conductivity still decreases at $y > 2$, this may suggest that Cu atoms are transformed from acceptors to donors as the Cu concentration is increased, i.e., the Cu atoms are ionized and start compensating for themselves[12] in the form of Cu$^+$ and/or Cu^{2+}. Such phenomena may take place because hole-donating (Cu^{-1}) and electron-donating (Cu$^+$/Cu^{2+}) Cu ions may exist, i.e., among the three kinds of impurity sites in β-rhombohedral B (Sec. III A), cation and anion favorable sites can exist for Cu-doped β-rhombohedral B. This hypothesis is discussed further based on our magnetic-susceptibility results.

C. Magnetic susceptibility

Figure 5 shows the temperature dependence of magnetic susceptibility χ for Li- and Cu-doped β-rhombohedral B, where it should be noted that these results are essentially similar to corresponding ones
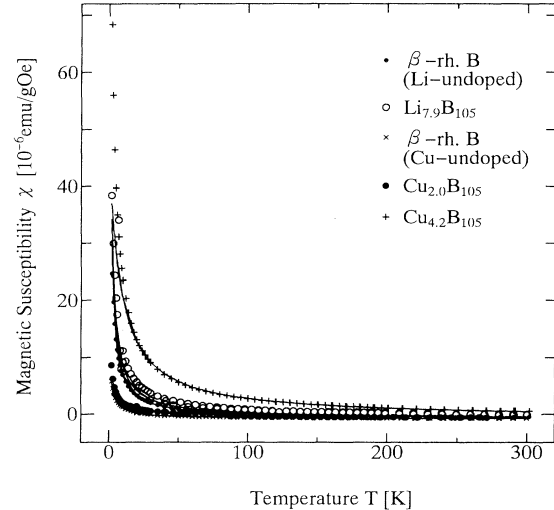
FIG. 5. Temperature dependence of magnetic susceptibility χ for Li-doped β-rhombohedral B polycrystals, arc-melted Cu-doped β-rhombohedral B polycrystals, and single-crystalline Cu$_{4.2}$B$_{105}$, being described by the temperature-independent component χ_0 and Curie-Weiss–type paramagnetic component χ_{CW}. Note that χ for a pristine β-rhombohedral B polycrystal (raw material for Li doping) and arc-melted pristine β-rhombohedral B polycrystal (raw material for Cu doping) are also shown. The solid lines indicate fitted $\chi = \chi_0 + C/(T - \Theta)$.

for single-crystalline Cu- and Al-doped β-rhombohedral B.[30] Namely, the χ versus T curves reveal the sum of the temperature-independent component χ_0 and Curie-Weiss–type paramagnetic component $\chi_{CW}[= C/(T - \Theta)]$ from 2 to 300 K. Thus, we calculated χ_0, Curie constant C, and Weiss temperature Θ by curve fitting. C is expressed as

$$C = N p_{\text{eff}}^2 / 3 k_B,$$

where N is the density of spin magnetic moment, p_{eff} the effective Bohr magneton per β-rhombohedral B unit cell (B_{105}), and k_B the Boltzmann constant. The dependence of χ_0 on the concentration x and y is respectively shown in Figs. 6(a) and 6(b), where if $N = 1$ per B_{105} applies to all samples, then the dependence of p_{eff} on x and y can also be calculated as indicated. Regarding χ_0,
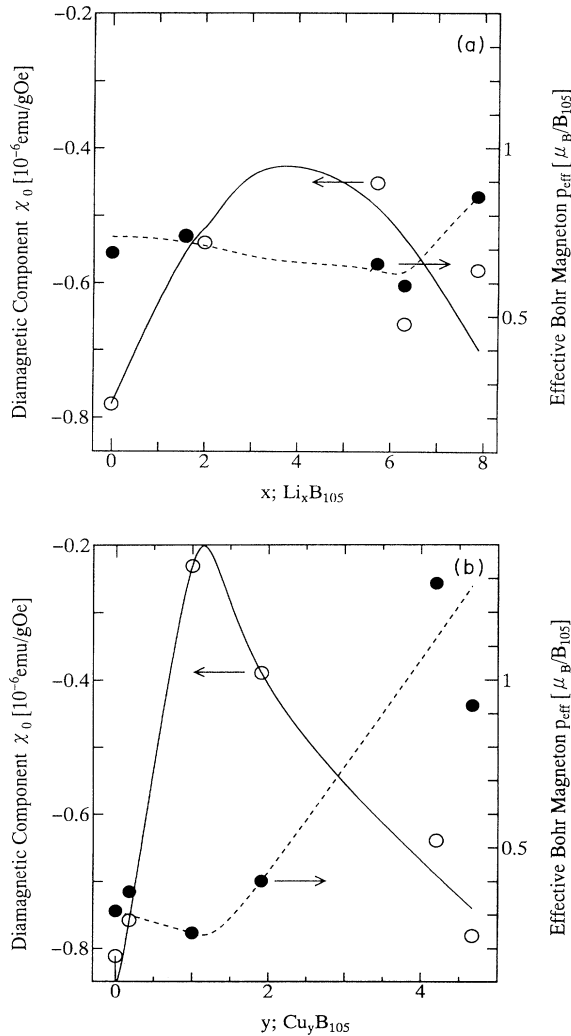
FIG. 6. Calculated magnetic parameters of temperature-independent component χ_0 and effective Bohr magneton per B_{105} rhombohedral unit cell p_{eff} for (a) Li-doped β-rhombohedral B polycrystals and (b) arc-melted Cu-doped β-rhombohedral B polycrystals. The solid and dashed lines assist viewing.

a paramagnetic peak occurs at $x \simeq 4$ and $y \simeq 2$, which deviates from the large diamagnetism present in pristine β-rhombohedral B ($\chi_0 \simeq -0.8 \times 10^{-6}$ emu/g Oe). In contrast, pristine fcc C_{60} shows a small χ_0 value, which is suggested to be responsible for the cancellation of ring current diamagnetism of π electrons, and the Van Vleck paramagnetism caused by the difference between the highest occupied molecular orbital and lowest unoccupied molecular orbital of the C_{60} molecule.[31] Since χ_0 reflects contributions of Pauli paramagnetism from conduction electrons (or holes) and core/orbital diamagnetism, the observed paramagnetic shifts may indicate the existence of a metallic conducting phase. On the other hand, this may not be the case since the maximum value of $\Delta\chi_0 = 0.2 \times 10^{-6}$ emu/g Oe for $x \simeq 5$ and 0.5×10^{-6} emu/g Oe for $y \simeq 1$, both of which are relatively small in comparison with that for CsC_{60} having $\Delta\chi_0 = 0.8 \times 10^{-6}$ emu/g Oe.[32] It is known that the contribution from temperature-independent Van Vleck paramagnetism is often negligibly small in nonmagnetic elements; thus if it is assumed that the paramagnetic shifts are due to the sum of Pauli paramagnetism and Landau diamagnetism, then the DOS at the Fermi energy $N(E_F)_{\text{mag}}$ can be calculated using $\Delta\chi_0 = \frac{1}{3} g^2 \mu_B^2 N(E_F)_{\text{mag}}$. Accordingly, the apparent paramagnetic shift of $\Delta\chi_0 = 0.1 \times 10^{-6}$ emu/g Oe gives $N(E_F)_{\text{mag}} = 2.6$ states/eV B_{105}.

When the calculated values of $N(E_F)_{\text{mag}}$ from $\Delta\chi_0$ (Fig. 6) are compared with $N(E_F)$ values calculated from T_0 values of VRH-type $\sigma(T)$ (Fig. 4), they have the same order of magnitude and show a similar peak with respect to metal concentration. However, $\sigma(T)$ is not representative of being metallic since it showed characteristics of having severely localized carriers. Unfortunately, this similarity in $N(E_F)$'s cannot be presently explained. When the temperature dependence of Seebeck coefficient S was measured for Li- and Cu-doped β-rhombohedral B (data not shown), it was found that both show a metal-like linear temperature dependence and have a small value of ~ 50 μV/K at room temperature, which is much less than the corresponding value of ~ 10 mV/K for pristine β-rhombohedral B.[30] It should be noted that a similar temperature dependence and S value were observed for Na-doped Si_{136}, which showed VRH conduction.[27] On the other hand, no evidence of a metallic Drude-type spectrum[33] was observed for metal-doped β-rhombohedral B in the reflection spectra of ir and optical-absorption regions (data not shown), whereas a metallic spectrum has been observed in K_3C_{60}.[34]

The resultant χ_{CW} values indicate a weak antiferromagnetic interaction at $\Theta = -1$ to -5 K for all samples and for pristine β-rhombohedral B. However, those for polycrystalline $Cu_{4.7}B_{105}$ contrastingly showed a weak ferromagnetic interaction at $\Theta \simeq 1.7$ K. Of interest, p_{eff} appears to have a minimum value at the concentration where χ_0 showed a paramagnetic peak, and it markedly increases at $y = 4.2$. When considering this increase with (i) the observed dependence of $\sigma(T)$ on y [Fig. 4(b)], and (ii) the hypothesis that at $y < 2$ Cu atoms accept electrons (Cu^-), whereas at $y > 2$ the doped Cu atoms donate electrons such that ions of Cu^+ and/or Cu^{2+} are formed, then it seems reasonable to conclude that the ob-

served magnetic moment may have originated from the Cu^{2+} ions.

IV. CONCLUSIONS

We have demonstrated that the main framework of β-rhombohedral B's crystalline structure is topologically similar to that of fcc C_{60}, and that their doping sites have similar dimensions. However, since β-rhombohedral B is comprised of covalently bound B_{12} icosahedral or B_{84} soccer-ball-shaped clusters, whereas fcc C_{60} is not, the electronic properties of metal-doped β-rhombohedral B are comparatively quite different. After doping β-rhombohedral B with Li and Cu atoms, the doped carriers showed metallic Pauli paramagnetism, whereas corresponding dc conductivity measurements contrastingly showed they possess VRH conduction between severely localized sites. On the other hand, the DOS at the Fermi energy, which was calculated using T_0 of VRH conduction, was found to have a similar dependence on concentration as that calculated from χ_0, with the value of DOS for Cu-doped β-rhombohedral B being consistent with the number of states originating from the intrinsic acceptor bands. Our most interesting finding is the existence of intrinsic acceptor bands and several kinds of doping sites, which when considered together, suggest that the sign of carriers and conduction mechanism of Li- and Cu-doped β-rhombohedral B are affected by some unknown, complex phenomenon.

* Present address: National Laboratory for High Energy Physics (KEK), Tsukuba, Ibaraki 305, Japan.

[1] D. Emin, Phys. Today **40**(1), 55 (1987).

[2] R. Frantz and H. Werheit, Europhys. Lett. **9**, 145 (1989).

[3] H. Werheit, M. Luax, and U. Kuhlmann, Phys. Status Solidi B **176**, 415 (1993).

[4] A. F. Hebert, M. J. Rosseinsky, R. C. Haddon, D. W. Murphy, S. H. Glarum, T. T. M. Palstra, A. P. Ramirez, and A. R. Kortan, Nature (London) **350**, 600 (1991).

[5] K. Holczer, O. Klein, S.-M. Huang, R. B. Kaner, K.-J. Fu, R. L. Whetten, and F. Diederich, Science **252**, 1154 (1991).

[6] M. J. Rosseinsky, A. P. Ramirez, S. H. Glarum, D. W. Murphy, R. C. Haddon, A. F. Hebard, T. T. M. Palstra, A. R. Kortan, S. M. Zahurak, and A. V. Mokhija, Phys. Rev. Lett. **66**, 2830 (1991).

[7] H. Kawaji, H. Horie, S. Yamanaka, and M. Ishikawa, Phys. Rev. Lett. **74**, 1427 (1995).

[8] S. Saito and A. Oshiyama, Phys. Rev. B **51**, 2628 (1995).

[9] S. Gunji, H. Kamimura, and T. Nakayama, J. Phys. Soc. Jpn. **62**, 2408 (1993).

[10] G. G. DeLeo, G. D. Watkins, and W. B. Fowler, Phys. Rev. B **25**, 4972 (1982).

[11] E. R. Weber, Appl. Phys. A **30**, 1 (1983).

[12] G. A. Slack, J. H. Rosolowski, C. Hejna, M. Garbauskas, and J. S. Kasper, in *Proceedings of the Ninth International Symposium on Boron, Boride, and Related Compounds*, edited by Helmut Werheit (University of Duisburg, Duisburg, 1987), p. 132.

[13] I. Higashi, M. Kobayashi, Y. Akagawa, K. Kobayashi, and J. Bernhard, in *Boron-Rich Solids*, edited by D. Emin, T. Aselage, A. C. Switendick, B. Morosin, and C. L. Beckel, AIP Conf. Proc. No. 231 (AIP, New York, 1991), p. 224.

[14] M. Kobayashi, I. Higashi, H. Matsuda, and K. Kimura, J. Alloys Comp. **221**, 120 (1995).

[15] B. Callmer, Acta Crystallogr. **33**, 1951 (1977).

[16] H. Werheit, H. Haupt, T. Lundström, and I. Higashi, Z. Naturforsch. Teil A **45**, 1016 (1990).

[17] Y. Maruyama, T. Inabe, H. Ogata, Y. Achiba, S. Suzuki, K. Kikuchi, and I. Ikemoto, Chem. Lett. **10**, 1849 (1991).

[18] X. D. Xiang, J.-G. Hou, G. Briceno, W. A. Vareka, R. Mostvoy, A. Zettel, V. H. Crespi, and M. L. Cohen, Science **256**, 1190 (1992).

[19] T. T. M. Palstra, R. C. Haddon, A. F. Hebard, and J. Zaanen, Phys. Rev. Lett. **68**, 1054 (1992).

[20] O. Klein and G. Grüner, Phys. Rev. B **46**, 11 247 (1992).

[21] A. F. Hebard, T. T. M. Palstra, R. C. Haddon, and R. M. Fleming, Phys. Rev. B **48**, 9945 (1993).

[22] M. P. Gelfand and J. P. Lu, Phys. Rev. Lett. **68**, 1050 (1992).

[23] K. Kimura, in Proceedings of 4th NEC Symposium on Fundamental Approaches to New Material Phases, edited by Y. Nishina, M. Mizuta, and H. Kamimura [Mater. Sci. Eng. B **19**, 67 (1993)].

[24] O. A. Golikova, N. Amandzhanov, M. M. Kazanin, G. M. Klimashin, and V. V. Kutasov, Phys. Status Solidi A **121**, 579 (1990).

[25] H. Werheit, U. Kuhlmann, R. Franz, W. Winkelbauer, B. Herstell, D. Fister, and H. Neisius, in *Boron-Rich Solids* (Ref. 13), p. 104.

[26] H. Werheit, U. Kuhlmann, and T. Tanaka, in *Boron-Rich Solids* (Ref. 13), p. 125.

[27] N. F. Mott, J. Solid State Chem. **6**, 348 (1973).

[28] N. F. Mott and E. A. Davis, *Electronic Processes in Non-Crystalline Materials* (Clarendon, Oxford, 1979).

[29] R. F. Milligan, T. F. Rosenbaum, R. N. Bhatt, and G. A. Thomas, in *Electron-Electron Interaction in Disordered Systems*, edited by A. L. Efros and M. Pollak (North-Holland, Amsterdam, 1985), p. 231.

[30] H. Matsuda, T. Nakayama, K. Kimura, H. Ino, Y. Murakami, H. Suematsu, and I. Higashi, in Proceedings of the 11th International Symposium on Boron, Borides, and Related Compounds, 1993, edited by R. Uno and I. Higashi

[Jpn. J. Appl. Phys. Series **10**, 39 (1994)].

[31] V. Elser and R. C. Haddon, Phys. Rev. A **36**, 4579 (1987).

[32] H. Suematsu, Y. Murakami, T. Arai, K. Kikuchi, Y. Achiba, and I. Ikemoto, Mater. Sci. Eng. B **19**, 141 (1993).

[33] H. Werheit, R. Schmechel, K. Kimura, H. Matsuda, and T. Nakayama (unpublished).

[34] Y. Iwasa, K. Tanaka, T. Yasuda, T. Koda, and S. Koda, Phys. Rev. Lett. **69**, 2284 (1992).